Cell genomics and immunosuppressive biomarker expression influence PD-L1 immunotherapy treatment responses in HNSCC—a computational study

Amber M. Bates, BS,[a] Emily A. Lanzel, DDS, MS,[b] Fang Qian, PhD,[a,c] Taher Abbasi, ME, MBA,[d] Shireen Vali, PhD,[d] and Kim A. Brogden, PhD[a]

Objectives. Programmed death—ligand 1 (PD-L1) expression is correlated with objective response rates to PD-1 and PD-L1 immunotherapies. However, both immunotherapies have only demonstrated 12%-24.8% objective response rates in patients with head and neck squamous cell carcinoma (HNSCC), demonstrating a need for a more accurate method to identify those who will respond before their therapy. Immunohistochemistry to detect PD-L1 reactivity in tumors can be challenging, and additional methods are needed to predict and confirm PD-L1 expression. Here, we hypothesized that HNSCC tumor cell genomics influences cell signaling and downstream effects on immunosuppressive biomarkers and that these profiles can predict patient clinical responses.

Study Design. We identified deleterious gene mutations in SCC4, SCC15, and SCC25 and created cell line—specific predictive computational simulation models. The expression of 24 immunosuppressive biomarkers were then predicted and used to sort cell lines into those that would respond to PD-L1 immunotherapy and those that would not.

Results. SCC15 and SCC25 were identified as cell lines that would respond to PD-L1 immunotherapy treatment and SCC4 was identified as a cell line that would not likely respond to PD-L1 immunotherapy treatment.

Conclusions. This approach, when applied to HNSCC cells, has the ability to predict PD-L1 expression and predict PD-1- or PD-L1-targeted treatment responses in these patients. (Oral Surg Oral Med Oral Pathol Oral Radiol 2017;124:157-164)

Programmed death—ligand 1 (PD-L1) is a 33.28-kDa protein on the surface of many immune and nonimmune cells and serves as a co-stimulatory molecule to regulate immune responses.[1-3] Overexpression of PD-L1 on tumor cells skews anti-tumor immunity by impeding anti-tumor CD8+ T-cell function through inhibition of T-cell proliferation, reduction of T-cell survival, inhibition of cytokine release, and promotion of T-cell apoptosis.[4,5]

PD-L1 has become an important marker in immunotherapy, and progress has been made to show that PD-L1 is an important clinical predictor of immunotherapy treatment success. Unfortunately, progress has lagged in the development of new methods to adequately detect PD-L1 expression on cells and in tumors. The expression of PD-L1 in tumors is currently determined by antibody-based tests, including immunohistochemistry (IHC),[6] quantitative immunofluorescence,[6] and antibodies conjugated with DOTAGA and radiolabeled with copper-64 for positron emission tomography—computed tomography imaging.[7] In IHC, PD-L1 levels of reactivity above a 1%-5% threshold for PD-L1$^+$ tumors are used for selecting patients for anti-PD-1 or anti-PD-L1 immunotherapy treatment.[8,9] Unfortunately, anti-PD-1 and anti-PD-L1 immunotherapy treatments have only demonstrated 12%-24.8% objective response rates (Table I). Several other studies are currently ongoing.[10] Using additional methods to detect PD-L1 expression could result in higher PD-L1 detection rates and higher patient objective response rates.

In this study, we hypothesized that HNSCC tumor cell genomics influences cell signaling and downstream

Statement of Clinical Relevance

This study reports translational research with clinical applications showing the feasibility of creating computational models. Our approach has the ability to accurately predict programmed death—ligand 1 (PD-L1) expression, affirm immunohistochemistry results, and determine PD-1— or PD-L1—targeted treatment responses in patients with head and neck squamous cell carcinoma.

Kim A. Brogden has had a Cooperative Research and Development Agreement with Cellworks Group Inc., San Jose, CA. Amber M. Bates, Emily A. Lanzel, and Fang Qian, declare that they have no conflict of interest. Taher Abbasi and Shireen Vali are employed by Cellworks Group Inc., San Jose, CA.

This work was supported by the National Institutes of Health grants R01 DE014390 and T90 DE023520.

[a]Iowa Institute for Oral Health Research, College of Dentistry, University of Iowa, Iowa City, IA, USA.
[b]Department of Oral Pathology, Radiology and Medicine, College of Dentistry, University of Iowa, Iowa City, IA, USA.
[c]Division of Biostatistics and Research Design, College of Dentistry, University of Iowa, Iowa City, IA, USA.
[d]Cellworks Group, Inc., San Jose, CA, USA.

Received for publication Jan 10, 2017; returned for revision May 9, 2017; accepted for publication May 9, 2017.

2212-4403
http://dx.doi.org/10.1016/j.oooo.2017.05.474

Table I. Objective response rates in HNSCC trials assessing antibodies against PD-1 and PD-L1

Checkpoint inhibitor study (Reference)	*Objective response "responder rate" (No. of patients)*	*Calculated "nonresponder rate"*
PD-1		
Pembrolizumab (MK-3475)[9,49]	19.6% (56)	80.4%
Pembrolizumab (MK-3475)[50]	24.8% (150)	75.2%
Nivolumab (BMS-936558)[9,17,50]	Study is ongoing	
Pidilizumab (CT-011)[9,17]	Study is ongoing	
PD-L1		
MPDL3280 A[51]	20.5% (122)	79.5%
MEDI4736[52]	14.0% (22)	86.0%
Durvalumab (MEDI4736)[50,53]	12.0% (62)	88.0%

HNSCC, head and neck squamous cell carcinoma; *PD-1,* programmed death 1; *PD-L1,* programmed death−ligand 1.

effects on the expression of PD-L1, chemokines, and immunosuppressive biomarkers and that these profiles can be used to predict clinical responses in patients.

To show this, we first identified deleterious gene mutation profiles in the American Type Culture Collection cell lines SCC4, SCC15, and SCC25. Then, we annotated these profiles into a cancer network to create cell line−specific predictive computational simulation models. Cell-specific models were used to predict the expression of 24 chemokines and immunosuppressive biomarkers. The profile results were finally used to sort cell lines into those that would respond to PD-L1 immunotherapy and those that would not. This approach would have the ability to predict PD-L1 expression, affirm IHC results, and accurately determine PD-1− or PD-L1−targeted treatment success.

MATERIAL AND METHODS

HNSCC cell line authentication

This was a predictive computational study, and cell lines were *not* used directly in this study.

Cell line mutational profiles

SCC cell line−specific mutational profiles were first created, as recently described.[11] Next-generation sequencing information containing mutations and copy number variations were taken from the cBioPortal for Cancer Genomics database[12,13] and from the Sanger sites for SCC4 (http://www.cbioportal.org/case.do?sample_id=SCC4_UPPER_AERODIGESTIVE_TRACT&cancer_study_id=cellline_ccle_broad, http://cancer.sanger.ac.uk/cell_lines/sample/overview?id=910904); SCC15 (http://www.cbioportal.org/case.do?sample_id=SCC15_UPPER_AERODIGESTIVE_TRACT&cancer_study_id=cellline_ccle_broad, http://cancer.sanger.ac.uk/cell_lines/sample/overview?id=910911); and SCC25 (http://www.cbioportal.org/case.do?sample_id=SCC25_UPPER_AERODIGESTIVE_TRACT&cancer_study_id=cellline_ccle_broad, http://cancer.sanger.ac.uk/cell_lines/sample/overview?id=910701).

Exomes from each cell line were examined for deleterious gene mutations, as recently described,[11] using cancer mutation effect prediction algorithms, including FannsDB,[14] SIFT,[15] Polyphen,[16] FATHMM,[14] Mutation Assessor,[17] and PROVEAN.[18] Final results after sifting the gene mutations through these algorithms were recorded as an effect of unknown significance, of neutral significance, or deleterious to gene function.[11]

Simulation models

An extensive cancer network was used to create predictive computational simulation models of SCC4, SCC15, and SCC25, as recently described.[11] This network was created from published reports on cell receptors, signaling pathways, pathway signaling intermediates, activation factors, transcription factors, and enzyme kinetics (Figure 1). Information on gene functionality and links between different genes, proteins, and pathways were manually researched, analyzed, curated, and aggregated to construct the integrated network maze. This approach modeled protein−protein interactions at each step in a signaling pathway using ordinary differential equations (ODEs)[19] to predict specific pathway output.[20] Pathway protein−protein interactions at each specific node were modeled as Michaelis-Menten equations that contained the reaction, enzyme, initial concentrations of protein intermediate reactants, and parameters of the reaction like Ka, Km, kcat, Vmax, etc. ODEs were solved at each step using the Radau method.[21] Modeled events included, but were not limited to, interactions at the cell surface (e.g., binding of agonists to receptors, etc.), metabolic and cell signaling pathways (e.g., signal pathway events, cross-talk interactions among pathways, feedback control, etc.), activation and regulation of genes (e.g., activation links of transcription factors, etc.), and intracellular processes (e.g., proteasomal degradation, endoplasmic reticulum stress, oxidative stress, DNA damage and repair pathways, and cell cycle pathways). Time-dependent changes in signaling pathway fluxes of biologic reactions were determined using modified ODEs solved with a proprietary solver. Input, output, and interactions in this network were validated using internal control analysis checks on predictive expression. Analyses included assessing the effects of pathway molecule overexpression or knockdown on predictive pathway responses; effects of drugs on

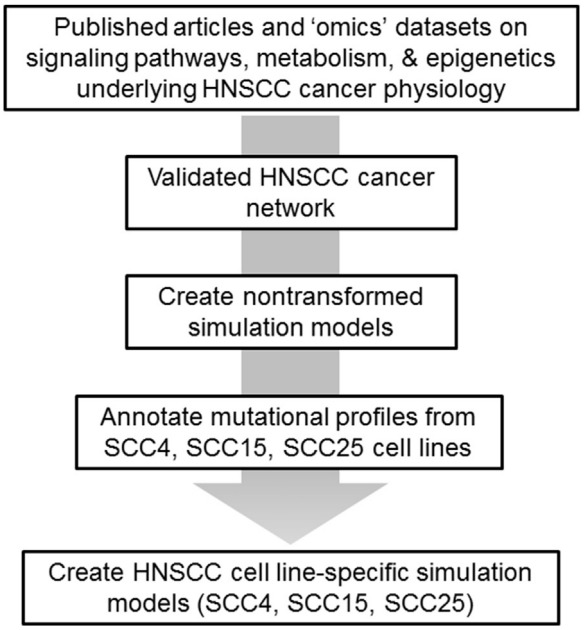

Fig. 1. The schema showing the creation of SCC4-, SCC15-, and SCC25-specific predictive computational simulation models. Information from manual review of new and published research was used to form the cancer network. Data was organized into signaling, metabolic, and epigenetic pathways to form the basis of the mathematical modeling of the cancer network. Nontransformed head and neck squamous cell carcinoma (HNSCC) models in the cancer network (e.g., models not containing cell line–specific deleterious gene mutations) were simulated to reach a control baseline. Cell line–specific deleterious gene mutation profiles were converted into a computational format and annotated into the HNSCC cancer network and simulated to create SCC4-, SCC15-, and SCC25-specific simulation models. These models were used to predict the expression of 24 chemokines and immunosuppressive biomarkers for SCC4, SCC15, and SCC25.

predictive pathway responses; and activation, regulation, and cross-talk interactions among pathway intermediates on predictive pathway responses.

HNSCC-specific models in the cancer network were created for each cell line. At the initial step, the models did not contain cell line–specific deleterious gene mutation profiles and were simulated to reach a homeostatic steady state, which served as the control baseline for the biomarkers of interest. Then, cell line–specific deleterious gene mutation profiles were converted into a computational format and annotated into the HNSCC cancer network, simulated to induce the cell line–specific cancer disease states, and used to predict the expression of 24 chemokines and immunosuppressive biomarkers. At the network level, mutations of oncogenes were represented as gain of function at the activity level, and mutations of tumor suppressor genes were represented as loss of function at the activity level unless explicit functionality of the mutation was known from published studies. Copy number variations, such as amplifications and deletions, were represented as overexpression or deletion of function at the expression level. The time required to achieve a cell line–specific network varied, depending on the complexity of the profile definition.

Table II. The predicted expression of chemokines compiled into a DC infiltration index

Chemokine	*SCC4 (%)*	*SCC15 (%)*	*SCC25 (%)*
CCL11	−3.61	5.84	3.61
CCL20	−0.26	7.06	4.73
CCL2	−10.22	18.12	7.62
CCL3	−2.10	2.54	0.65
CCL4	21.53	25.58	4.44
CCL5	−2.91	3.53	1.95
CCL7	−3.69	6.73	4.08
CX3 CL1	−0.79	5.57	3.45
CXCL14	−0.89	−0.83	−1.16
DC infiltration index	**−2.95**	**74.14**	**29.37**

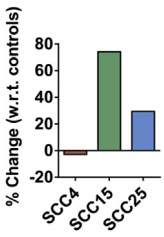

DC, dendritic cell; *w.r.t.,* with respect to.
The percent change was calculated for each chemokine as ([D − C]/C) × 100, where C is the predicted baseline value of the nontumorigenic control (μM), and D is the predicted disease value of the biomarker obtained in the cell line–specific network (μM). The chemokines were given weightage to normalize the total to 1. The index was calculated to be the sum of each prediction percentage change × weightage.

Immunosuppressive biomarkers

The predicted expression of 24 biomarkers were determined, including PD-L1, 9 chemokines capable of trafficking dendritic cells into the tumor microenvironment[22,23] (Table II; Figure 2), and 14 biomarkers that can act as immunosuppressive mediators facilitating the ability of cancer cells to escape normal tumor surveillance (Table III). Expression was reported as percent change (with respect to control) and calculated as ([D - C]/C) × 100, where C is the absolute value of the nontumorigenic baseline control (μM), and D is the absolute value of the biomarker obtained in the cell line–specific cancer state network (μM). Chemokine percent expression values were given weightage so as to normalize the total to 1. A dendritic cell infiltration index was then calculated to be the sum of each prediction percentage change × weightage (Table II).

Predicted response to PD-L1 immunotherapy

The predicted expression of 24 chemokines and immunosuppressive biomarkers were used to sort cell lines into those that would respond to PD-L1 immunotherapy and those that would not (Figure 2). Predetermined thresholds were assigned to each step.

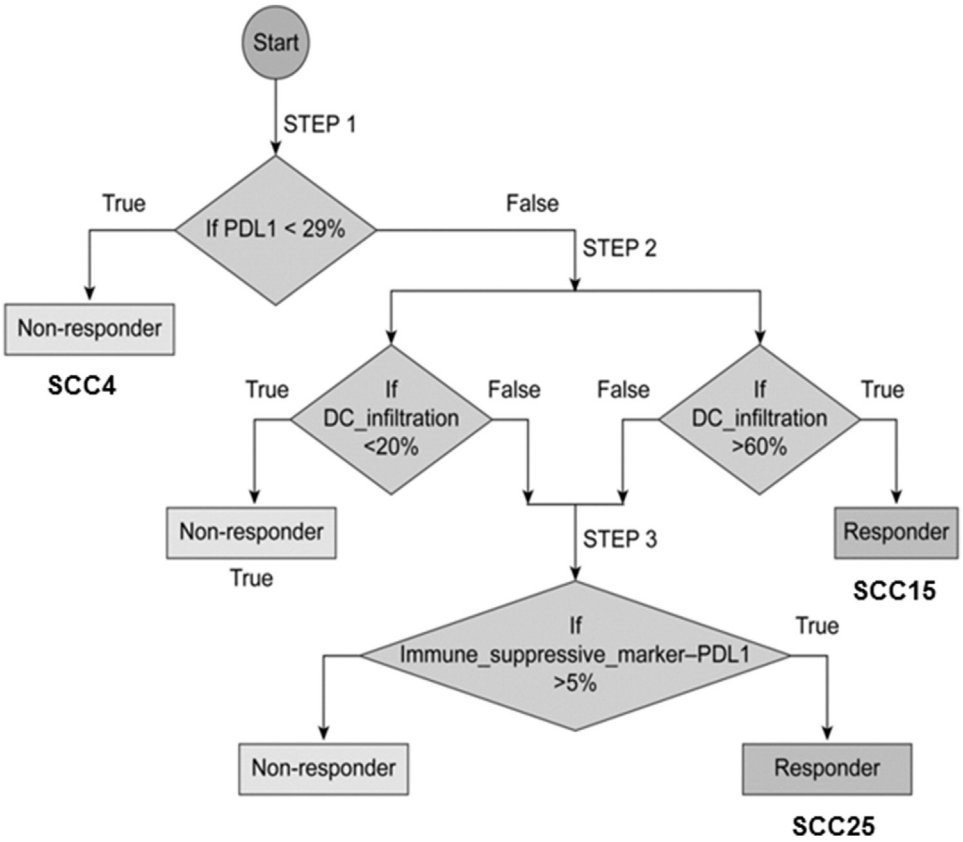

Fig. 2. The predicted expression profiles of 24 chemokines and immunosuppressive biomarkers for SCC4, SCC15, and SCC25 were used in a decision tree format to sort cell lines into those that would likely respond to PD-L1 immunotherapy treatment and those that would not. SCC4 had 11.14% programmed death−ligand 1 (PD-L1) expression and was identified at step 1 as a cell line that would not likely respond to PD-L1 immunotherapy treatment. SCC15 had a dendritic cell (DC) infiltration index of 74.11% and was identified at step 2 as a cell line that would likely respond to PD-L1 immunotherapy treatment. SCC25 had immunosuppressive biomarker expression (ranging from −4.96% for Fas ligand gene [FASLG] to 42.45% for interleukin-6 [IL-6]) with <91.38% PD-L1 expression plus 5% and was identified at step 3 as a cell line that would likely respond to PD-L1 immunotherapy treatment.

In step 1, a 29% PD-L1 expression threshold was used. Cell lines with PD-L1 expression <29% were classified as PD-L1 immunotherapy nonresponders. Cell lines with PD-L1 expression >29% moved on to the next step.

In step 2, both 20% and 60% dendritic cell infiltration index thresholds were used. Cell lines with a dendritic cell infiltration index <20% were classified as PD-L1 immunotherapy nonresponders. Cell lines with a dendritic cell infiltration index >60% were classified as PD-L1 immunotherapy responders. Cell lines with a dendritic cell index >20% and <60% moved on to the final step.

In step 3, the cell line−specific PD-L1 expression with a margin of >5% threshold was used. Cell line immunosuppressive biomarker predictions greater than the cell line−specific PD-L1 expression with a margin of >5% were classified as PD-L1 immunotherapy nonresponders. Cell line immunosuppressive biomarker predictions less than the cell line−specific PD-L1 expression with a margin of >5% were classified as PD-L1 immunotherapy responders.

RESULTS

Predictions of biomarkers

The predicted expression of 24 chemokines and immunosuppressive biomarkers varied among the 3 cell lines (Tables II and III). PD-L1 expression varied from 11.14% (SCC4) and 49.29% (SCC15) to 91.38% (SCC25) (Table III). The percentage changes of PD-L1 expression with respect to control baselines were previously verified against observed PD-L1 expression by using enzyme-linked immunosorbent assay, IHC, and flow cytometry on the same cells grown in culture.[11]

The expression of chemokines for SCC4 ranged from −10.22% for CCL2 to 21.53% for CCL4 (Table II). In 8 of 9 chemokine predictions, the

Table III. The predicted expression of PD-L1, dendritic cell infiltration index, and immunosuppressive biomarkers from simulation models of SCC4, SCC15, and SCC25

Markers and index	*SCC4 (%)*	*SCC15 (%)*	*SCC25 (%)*
PD-L1*	11.14	49.29	91.38
Dendritic cell infiltration index	−2.93	74.11	29.38
Immunosuppressive biomarkers			
TGF-β1	5.66	58.8	24.38
IDO1	17.29	2.75	4.97
IL-6	−8.49	406.78	42.45
VEGFA	44.18	78.23	26.78
TDO2	2.74	2.39	18.29
PGE_2	39.04	39.19	26.97
IL-10	2.01	46.53	26.09
LGALS9	−49.72	5.15	10.82
FASLG	−1.05	−2.98	−4.96
CD47	5.36	14.39	8.21
CTLA-4	27.89	80.37	10.38
PDCD1 LG2	3.6	7.89	5.65
Ganglioside GM3	−4.39	48.69	36.44
Ganglioside GD2	−4.39	48.69	36.44

PD-L1, programmed death−ligand 1; *TGF,* transforming growth factor; *IDO1,* indoleamine 2,3-dioxygenase 1; *IL,* interleukin; *VEGFA,* vascular endothelial growth factor A; *TDO2,* tryptophan 2,3-dioxygenase 2; *PGE_2,* prostaglandin E_2; *LGALS9,* lectin, galactoside-binding, soluble, 9; *FASLG,* fas ligand gene; *CTLA-4,* cytotoxic T-lymphocyte-associated protein 4; *PDCD1 LG2,* Programmed Cell Death 1 Ligand 2.

Values are listed as percent expression with respect to controls.

*The percentage changes of PD-L1 expression were previously reported and verified against observed PD-L1 expression by enzyme-linked immunosorbent assay, immunohistochemistry, and flow cytometry on the same cells grown in culture.[11]

percentage changes were lower than in the control baselines. The percentage changes for SCC15 ranged from −0.83% for CXCL14 to 25.58% for CCL4. The percentage changes for SCC25 ranged from −1.16% for CXCL14 to 7.62% for CCL2. These variations resulted in differences in the predicted dendritic cell infiltration index values (Table II). These index values varied from −2.93% (SCC4) and 29.36% (SCC25) to 74.11% (SCC15) (Table III).

The expression of immunosuppressive biomarkers for SCC4 ranged from −49.72% for LGALS9 (Lectin, Galactoside-Binding, Soluble, 9) to 44.18% for vascular endothelial growth factor (VEGF) A (Table III). The percentage changes of immunosuppressive biomarkers for SCC15 ranged from −2.98% for Fas ligand gene (FASLG) to 406.78% for interleukin (IL)-6 and the percentage changes for SCC25 ranged from −4.96% for FASLG to 42.45% for IL-6.

Predicted response to PD-L1 immunotherapy

The predicted expression of 24 chemokines and immunosuppressive biomarkers for SCC4, SCC15, and SCC25 were used to sort cell lines into those that would respond to PD-L1 immunotherapy treatment and those that would not (Figure 2).

SCC4 had 11.14% predicted PD-L1 expression, SCC15 had 49.29% predicted PD-L1 expression, and SCC25 had 91.38% predicted PD-L1 expression (Table III). In step 1, SCC4 was classified as a PD-L1 immunotherapy nonresponder. SCC15 and SCC25 cell lines moved on to the next step.

SCC15 had a 74.11% predicted dendritic cell infiltration index, and SCC25 had a 29.38% predicted dendritic cell infiltration index (Tables II and III). In step 2, SCC15 was classified as a PD-L1 immunotherapy responder. SCC25 cell line moved on to the next step.

SCC25 had an immunosuppressive biomarker expression profile ranging from −4.96% for FASLG to 42.45% for IL-6 (Table III). All of these profile predicted values were less than the 91.38% PD-L1 expression plus 5%. In step 3, SCC25 was classified as a PD-L1 immunotherapy responder.

Predicted pathway comparisons

In our previous study, deleterious gene mutations involved in the expression of PD-L1 in SCC4, SCC15, and SCC25 cell lines were mapped to unique signaling pathways.[11] To show that cell genomics influenced immunosuppressive biomarker expression profiles, we mapped mutations to unique signaling pathways. Deleterious gene mutations involved in the expression of PD-L1, 9 chemokines, and 14 immunosuppressive biomarkers for SCC4 were mapped to signaling networks TP53, CDK6, CCND1, and NF1. Mutations in SCC15 were mapped to signaling networks EGFR, PIK3 CB, DUSP22, and MAP3 K1, and mutations in SCC25 were mapped to signaling networks TP53, CDKN2 A, and LAMTOR5.

DISCUSSION

Recently, we developed an approach to determine the expression levels of PD-L1 in SCC4, SCC15, and SCC25 cell lines.[11] The percentage changes of PD-L1 expression were verified against observed PD-L1 expression using enzyme-linked immunosorbent assay, IHC, and flow cytometry on the same cells grown in culture.[11] In this study, we extended that methodology and determined the expression levels of 24 chemokines and immunosuppressive biomarkers. The expression levels of individual chemokines were converted into an index of dendritic cell infiltration. All of these values were then used to show that SCC15 and SCC25, cell lines originally from patients with HNSCC, would likely respond to PD-L1 immunotherapy treatment and that SCC4, a cell line from a

patient with HNSCC, would not likely respond to PD-L1 immunotherapy treatment. These differences were based on cell genomics and immunosuppressive biomarker expression profiles from each cell line influenced by cell specific mutations, copy number variations, and methylation data.

Predicting responses to PD-L1 immunotherapy treatment of patients with HNSCC is generally determined using IHC to identify PD-L1 reactivity in tumors. This reactivity, if above predetermined thresholds, is then used to select patients for PD-1 or PD-L1 immunotherapy treatment.[8,9,24] However, IHC to detect PD-L1 has come under some scrutiny and can be imprecise.[6,25-28] IHC is complicated, in part, by the variability in available reagents,[28,29] and this variability presents challenges for using PD-L1 reactivity in IHC alone as both a diagnostic marker and as a clinical predictor of PD-L1 immunotherapy treatment success.

Complex input from tumor mutations, inflammatory cells, and immunosuppressive biomarkers likely contributes to the production and regulation of PD-L1.[29-31] Many of these concepts were included in our choice of a multifaceted biomarker system. These concepts were also included in the cut-off points used to predict PD-L1 immunotherapy responder status in the decision tree (Figure 2). The 24 biomarkers (Tables II and III) were not chosen arbitrarily, but for their suggested roles in tumor progression. PD-L1 was included because it is expressed in 46%-100% of human HNSCC biopsy specimens across multiple primary sites.[32]

Decision cut-offs were established but not limited to those included in Figure 2. In a recent study of unpublished results,[33] cut-offs for the predicted PD-L1 expression (step 1), the predicted dendritic cell infiltration index (step 2), and the predicted immunosuppressive biomarker profile (step 3) were used to predict PD-1 immunotherapy responder status of patients with non−small cell lung cancer. The decision tree was found to be robust with built-in redundancy. Basing the PD-1 drug responder status on 3 separate predicted criteria allowed a PD-1 immunotherapy responder/nonresponder not identified at one step to be identified at a later step. In addition, the thresholds were specific. Using non−small cell lung cancer as the model,[34] decreasing the PD-L1 expression cut-off from 29% to 25% identified 6 non−PD-1 responders as opposed to the identification of 9 PD-1 nonresponders at 29%. Increasing the PD-L1 expression cut-off from 29%-35% identified more false negatives, and setting the PD-L1 drug responder status at 35% identified up to 13 PD-1 nonresponders (3 PD-1 responders were identified as PD-1 nonresponders).

Altered chemokine function in HNSCC promotes cell survival, enhanced proliferation, neovascularization, motility, and metastasis in multiple tumor types.[35] Therefore, 9 predicted chemokines were used to generate an index representative of the trafficking of dendritic cells into the tumor microenvironment.[22,23] Transforming growth factor-β from tumor cells impairs the function of dendritic cells and T cells needed for tumor recognition and antitumor responses.[36,37] Transforming growth factor-β is overexpressed in HNSCC development and decreases expression of interferon-gamma (IFN-γ) on cytotoxic T lymphocytes.[36-38] Indoleamine 2,3-dioxygenase (IDO) 1, a tryptophan degrading enzyme, inhibits the proliferation of lymphocytes; acts on natural killer (NK) cells to downregulate receptors and induces NK-cell apoptosis; and acts on cytotoxic T cells to induce cell cycle arrest, decrease activation, and apoptosis.[39-43] IDO is expressed in a variety of human cancers; in HNSCC, IDO has been suggested to play a role in IFN-γ−induced apoptosis.[44]

Tryptophan 2,3-dioxygenase 2, another tryptophan-degrading enzyme involved in immune resistance, is frequently expressed in human cancers.[39] In breast cancer, tryptophan 2,3-dioxygenase 2 is highly overexpressed and is believed to contribute to tumor progression and poor prognosis.[45] IL-6 is involved in inflammatory processes indicative of tumor proliferation, has immunosuppressive effects on dendritic cells, and prevents maturation.[37,46] Expression of IL-6 in HNSCC cells has been suggested as a predictive factor of poor response to chemoradiotherapy.[47] VEGF is a marker for tumor invasion and metastasis and can be detected in HNSCC.[37] It promotes immune tolerance and angiogenesis.[36] Higher levels of IL-6 and VEGF are produced in late-stage HNSCC cell lines compared with early-stage cell lines and in metastatic cell lines compared with nonmetastatic cell lines.[37] Prostaglandin E_2 (PGE_2) suppresses NK-cell function primarily through the PGE_2 receptor EP_4.[48] IL-10 is found in elevated levels in the saliva of patients with HNSCC and may impair dendritic cell function and protect tumor cells from cytotoxic T cells.[38,49,50] LGALS9 encodes for galectin-9, which is associated with metastasis and immunosuppression and found in elevated levels of lung, kidney, liver, and breast carcinomas.[51] Galectin-9 has been suggested to play a role in tumor cell evasion by inducing apoptosis in T helper 1 cells and cytotoxic T cells. It mediates T-cell dysfunction and T-cell senescence.[52] FASLG triggers Fas-mediated apoptosis and is overexpressed in various types of tumors.[53] Tumor cells can express FASLG and induce apoptosis in T cells expressing Fas, allowing for tumor progression. CD47 represses dendritic cell phagocytosis, maturation, and production of IFN-γ.[54] Cytotoxic T-lymphocyte-associated protein 4 restrains the adaptive immune response of T cells toward tumor-associated

antigens.[55-57] Programmed Cell Death 1 Ligand 2 encodes for PD-L2 (programmed death 1 ligand-2), which is expressed by tumor cells to bind PD-1 on effector T cells thereby suppressing antitumor cellular immunity similar to PD-L1.[58] PD-L2 is commonly expressed in cervical SCC. Gangliosides GM3 and GD2 impair dendritic cell differentiation from monocytes and induce their apoptosis.[59]

CONCLUSIONS

In summary, we used a goal-orientated, translational approach to create HNSCC-specific simulation models to predict PD-L1 immunotherapy outcomes using deleterious gene mutation profiles from 3 American Type Culture Collection SCC cell lines of head and neck origin. This approach was modeled and has the potential to complement PD-L1/PD-1-targeted drug responder status predictions determined by the current methods used. In future studies, the predicted responder status will be validated in clinical trials for HNSCC, where cell line−specific deleterious gene mutations, PD-L1 IHC reactivity of tumors, and clinical outcomes are available. Simulation models have a strong potential for future applications. These models will be able to complement IHC results or provide effective where IHC is unfeasible, identify factors that influence PD-L1 expression, and serve as a clinical decision support system to classify patients into those that would respond to PD-L1 immunotherapy and those that would not. The last-mentioned application could be used shortly after cancer diagnosis and just before cancer treatment to facilitate selection of appropriate therapies based on a patient's deleterious gene mutation profile.

REFERENCES

1. Francisco LM, Sage PT, Sharpe AH. The PD-1 pathway in tolerance and autoimmunity. *Immunol Rev*. 2010;236:219-242.
2. Pedoeem A, Azoulay-Alfaguter I, Strazza M, Silverman GJ, Mor A. Programmed death-1 pathway in cancer and autoimmunity. *Clin Immunol*. 2014;153:145-152.
3. Sharma P, Allison JP. The future of immune checkpoint therapy. *Science*. 2015;348:56-61.
4. Dong H, Strome SE, Salomao DR, et al. Tumor-associated B7-H1 promotes T-cell apoptosis: a potential mechanism of immune evasion. *Nat Med*. 2002;8:793-800.
5. Tseng SY, Otsuji M, Gorski K, et al. B7-DC, a new dendritic cell molecule with potent costimulatory properties for T cells. *J Exp Med*. 2001;193:839-846.
6. McLaughlin J, Han G, Schalper KA, et al. Quantitative assessment of the heterogeneity of PD-L1 expression in non-small-cell lung cancer. *JAMA Oncol*. 2016;2:46-54.
7. Lesniak WG, Chatterjee S, Gabrielson M, et al. PD-L1 Detection in tumors using [(64)Cu]atezolizumab with PET. *Bioconjug Chem*. 2016;27:2103-2110.
8. Taube JM, Klein A, Brahmer JR, et al. Association of PD-1, PD-1 ligands, and other features of the tumor immune microenvironment with response to anti-PD-1 therapy. *Clin Cancer Res*. 2014;20:5064-5074.
9. Sunshine J, Taube JM. PD-1/PD-L1 inhibitors. *Curr Opin Pharmacol*. 2015;23:32-38.
10. Economopoulou P, Perisanidis C, Giotakis EI, Psyrri A. The emerging role of immunotherapy in head and neck squamous cell carcinoma (HNSCC): anti-tumor immunity and clinical applications. *Ann Transl Med*. 2016;4:173.
11. Lanzel EA, Hernandez MPG, Bates AM, et al. Predicting PD-L1 expression on human cancer cells using next-generation sequencing information in computational simulation models. *Cancer Immunol Immunother*. 2016;65:1511-1522.
12. Gao J, Aksoy BA, Dogrusoz U, et al. Integrative analysis of complex cancer genomics and clinical profiles using the cBioPortal. *Sci Signal*. 2013;6:pl1.
13. Cerami E, Gao J, Dogrusoz U, et al. The cBio cancer genomics portal: An open platform for exploring multidimensional cancer genomics data. *Cancer Discov*. 2012;2:401-404.
14. Martelotto LG, Ng CK, De Filippo MR, et al. Benchmarking mutation effect prediction algorithms using functionally validated cancer-related missense mutations. *Genome Biol*. 2014;15:484.
15. Sim NL, Kumar P, Hu J, Henikoff S, Schneider G, Ng PC. SIFT web server: predicting effects of amino acid substitutions on proteins. *Nucleic Acids Res*. 2012;40(Web Server issue): W452-W457.
16. Adzhubei IA, Schmidt S, Peshkin L, et al. A method and server for predicting damaging missense mutations. *Nat Methods*. 2010;7:248-249.
17. Reva B, Antipin Y, Sander C. Predicting the functional impact of protein mutations: application to cancer genomics. *Nucleic Acids Res*. 2011;39:e118.
18. Choi Y, Sims GE, Murphy S, Miller JR, Chan AP. Predicting the functional effect of amino acid substitutions and indels. *PLoS One*. 2012;7:e46688.
19. Kholodenko BN, Demin OV, Moehren G, Hoek JB. Quantification of short term signaling by the epidermal growth factor receptor. *J Biol Chem*. 1999;274:30169-30181.
20. Kaushik P, Gorin F, Vali S. Dynamics of tyrosine hydroxylase mediated regulation of dopamine synthesis. *J Comput Neurosci*. 2007;22:147-160.
21. Hairer E, Wanner G. Stiff differential equations solved by Radau methods. *J Comput Appl Math*. 1999;111:93-111.
22. Balkwill F. Cancer and the chemokine network. *Nat Rev Cancer*. 2004;4:540-550.
23. Mukaida N, Sasaki S, Baba T. Chemokines in cancer development and progression and their potential as targeting molecules for cancer treatment. *Mediators Inflamm*. 2014;2014:170381.
24. Shukuya T, Carbone DP. Predictive markers for the efficacy of anti-PD-1/PD-L1 antibodies in lung cancer. *J Thorac Oncol*. 2016;11:976-988.
25. Philips GK, Atkins M. Therapeutic uses of anti-PD-1 and anti-PD-L1 antibodies. *Int Immunol*. 2015;27:39-46.
26. Kerr KM, Hirsch FR. Programmed death ligand 1 immunohistochemistry: friend or foe? *Arch Pathol Lab Med*. 2016;140:326-331.
27. Sholl LM, Aisner DL, Allen TC, et al; Members of Pulmonary Pathology Society. Programmed death ligand 1 immunohistochemistry − a new challenge for pathologists: a perspective from members of the pulmonary pathology society. *Arch Pathol Lab Med*. 2016;140:341-344.
28. Yu H, Boyle TA, Zhou C, Rimm DL, Hirsch FR. PD-L1 expression in lung cancer. *J Thorac Oncol*. 2016;11:964-975.
29. Bhaijee F, Anders RA. PD-L1 expression as a predictive biomarker: is absence of proof the same as proof of absence? *JAMA Oncol*. 2016;2:54-55.
30. Blank CU, Haanen JB, Ribas A, Schumacher TN. Cancer immunology. The "cancer immunogram". *Science*. 2016;352: 658-660.

31. Herbst RS, Soria JC, Kowanetz M, et al. Predictive correlates of response to the anti-PD-L1 antibody MPDL3280 A in cancer patients. *Nature*. 2014;515:563-567.
32. Zandberg DP, Strome SE. The role of the PD-L1:PD-1 pathway in squamous cell carcinoma of the head and neck. *Oral Oncol*. 2014;50:627-632.
33. Brogden KA, Parashar D, Hallier AR, et al. Computational simulation models containing NSCLC patient genomic signatures predict drug responder status to anti-PD-1 immunotherapy. In: *Proceedings of the 43rd International Society of Oncology and Biomarkers (ISOBM)*, Chicago, IL, September 1−6, 2016.
34. Rizvi NA, Hellmann MD, Snyder A, et al. Mutational landscape determines sensitivity to PD-1 blockade in non-small cell lung cancer. *Science*. 2015;348:124-128.
35. Sahingur SE, Yeudall WA. Chemokine function in periodontal disease and oral cavity cancer. *Fronts Immunol*. 2015;6:214.
36. Moutsopoulos NM, Wen J, Wahl SM. TGF-beta and tumors—an ill-fated alliance. *Curr Opin Immunol*. 2008;20:234-240.
37. Shkeir O, Athanassiou-Papaefthymiou M, Lapadatescu M, et al. In vitro cytokine release profile: Predictive value for metastatic potential in head and neck squamous cell carcinomas. *Head Neck*. 2013;35:1542-1550.
38. Rabinovich GA, Gabrilovich D, Sotomayor EM. Immunosuppressive strategies that are mediated by tumor cells. *Annu Rev Immunol*. 2007;25:267-296.
39. van Baren N, Van den Eynde BJ. Tumoral immune resistance mediated by enzymes that degrade tryptophan. *Cancer Immunol Res*. 2015;3:978-985.
40. Munn DH, Zhou M, Attwood JT, et al. Prevention of allogeneic fetal rejection by tryptophan catabolism. *Science*. 1998;281:1191-1193.
41. Lob S, Konigsrainer A, Rammensee HG, Opelz G, Terness P. Inhibitors of indoleamine-2,3-dioxygenase for cancer therapy: can we see the wood for the trees? *Nat Rev Cancer*. 2009;9:445-452.
42. Spranger S, Spaapen RM, Zha Y, et al. Up-regulation of PD-L1, IDO, and T(regs) in the melanoma tumor microenvironment is driven by CD8(+) T cells. *Sci Transl Med*. 2013;5:200ra116.
43. Iversen TZ, Andersen MH, Svane IM. The targeting of indoleamine 2,3 dioxygenase-mediated immune escape in cancer. *Basic Clin Pharmacol Toxicol*. 2015;116:19-24.
44. El Jamal SM, Taylor EB, Abd Elmageed ZY, et al. Interferon gamma-induced apoptosis of head and neck squamous cell carcinoma is connected to indoleamine-2,3-dioxygenase via mitochondrial and ER stress-associated pathways. *Cell Div*. 2016;11:11.
45. D'Amato NC, Rogers TJ, Gordon MA, et al. A TDO2-AhR signaling axis facilitates anoikis resistance and metastasis in triple-negative breast cancer. *Cancer Res*. 2015;75:4651-4664.
46. Hegde S, Pahne J, Smola-Hess S. Novel immunosuppressive properties of interleukin-6 in dendritic cells: inhibition of NF-κB binding activity and CCR7 expression. *FASEB J*. 2004;18:1439-1441.
47. Jinno T, Kawano S, Maruse Y, et al. Increased expression of interleukin-6 predicts poor response to chemoradiotherapy and unfavorable prognosis in oral squamous cell carcinoma. *Oncol Rep*. 2015;33:2161-2168.
48. Holt D, Ma X, Kundu N, Fulton A. Prostaglandin E(2) (PGE (2)) suppresses natural killer cell function primarily through the PGE(2) receptor EP4. *Cancer Immunol Immunother*. 2011;60:1577-1586.
49. Aziz S, Ahmed SS, Ali A, et al. Salivary immunosuppressive cytokines IL-10 and IL-13 are significantly elevated in oral squamous cell carcinoma patients. *Cancer Invest*. 2015;33:318-328.
50. Goncalves AS, Arantes DA, Bernardes VF, et al. Immunosuppressive mediators of oral squamous cell carcinoma in tumour samples and saliva. *Hum Immunol*. 2015;76:52-58.
51. Heusschen R, Schulkens IA, van Beijnum J, Griffioen AW, Thijssen VL. Endothelial LGALS9 splice variant expression in endothelial cell biology and angiogenesis. *Biochim Biophys Acta*. 2014;1842:284-292.
52. Li H, Wu K, Tao K, et al. Tim-3/galectin-9 signaling pathway mediates T-cell dysfunction and predicts poor prognosis in patients with hepatitis B virus-associated hepatocellular carcinoma. *Hepatology*. 2012;56:1342-1351.
53. Kim B, Lee HJ, Choi HY, et al. Clinical validity of the lung cancer biomarkers identified by bioinformatics analysis of public expression data. *Cancer Res*. 2007;67:7431-7438.
54. Ishii H, Tanaka S, Masuyama K. Therapeutic strategy for cancer immunotherapy in head and neck cancer. *Adv Cell Mol Otolaryngol*. 2015;3:27690.
55. Avogadri F, Yuan J, Yang A, Schaer D, Wolchok JD. Modulation of CTLA-4 and GITR for cancer immunotherapy. *Curr Top Microbiol Immunol*. 2011;344:211-244.
56. Mocellin S, Nitti D. CTLA-4 blockade and the renaissance of cancer immunotherapy. *Biochim Biophys Acta*. 2013;1836:187-196.
57. Grosso JF, Jure-Kunkel MN. CTLA-4 blockade in tumor models: an overview of preclinical and translational research. *Cancer Immun*. 2013;13:5.
58. Howitt BE, Sun HH, Roemer MG, et al. Genetic basis for PD-L1 expression in squamous cell carcinomas of the cervix and vulva. *JAMA Oncol*. 2016;2:518-522.
59. Peguet-Navarro J, Sportouch M, Popa I, et al. Gangliosides from human melanoma tumors impair dendritic cell differentiation from monocytes and induce their apoptosis. *J Immunol*. 2003;170:3488-3494.

Reprint requests:

Kim A. Brogden, PhD
Iowa Institute for Oral Health Research
N423 DSB, College of Dentistry
The University of Iowa, 801 Newton Road
Iowa City, IA 52242
USA
Kim-brogden@uiowa.edu